Quantifying primary and secondary source contributions to ultrafine particles in the UK urban background

S. M. L. Hama [1] [2], R. L. Cordell [1], and P. S. Monks [1]

[1] Department of Chemistry, University of Leicester, Leicester LE1 7RH, UK

[2] Department of Chemistry, School of Science, University of Sulaimani, Sulaimani, Iraq

Correspondence to: Paul S. Monks (psm7@le.ac.uk)

HIGHLIGHTS:

- Particle total number concentration (TNC) does not always reflect variations in traffic emissions
- Primary and secondary sources contribute in a seasonally variant and quantifiable way to particle number concentrations in Leicester.
- New particle formation was a significant contributor around midday to TNC in the Leicester urban atmosphere.
- In the Leicester urban atmosphere ultrafine particles are predominantly formed from secondary sources.

Keywords:

Ultrafine particles

Urban Background

Primary sources

Secondary sources

Abstract

Total particle number (TNC, ≥7 nm diameter), particulate matter ($PM_{2.5}$), equivalent black carbon (eBC) and gaseous pollutants (NO, NO_2, NOx, O_3, CO) have been measured at an urban background site in Leicester over two years (2014 and 2015). A derived chemical climatology for the pollutants showed maximum concentrations for all pollutants during the cold period except O_3 which peaked during spring. Quantification of primary and secondary sources of ultrafine particles (UFPs) was undertaken using eBC as a tracer for the primary particle number concentration in the Leicester urban area. At the urban background site, which is influenced by fresh vehicle exhaust emissions, TNC was segregated into two components, TNC = N1 + N2. The component N1 represents components directly emitted as particles and compounds which nucleate immediately after emission. The component N2 represents the particles formed during the dilution and cooling of vehicle exhaust emissions and by in situ new particle formation (NPF). The values of highest N1 (49%) were recorded during the morning rush hours (07:00-09:00 h), correlating with NOx, while the maximum contribution of N2 to TNC was found at midday (11:00-14:00 h), at around 62%, correlated with O_3. Generally, the percentage of N2 (57%) was greater than the percentage of N1 (43%) for all days at the AURN site over the period of the study. For the first time the impact of wind speed and direction on N1 and N2 was explored. The overall data analysis shows that there are two major sources contributing to TNC in Leicester: primary sources (traffic emissions) and secondary sources, with the majority of particles of secondary origin.

1. Introduction

Ultrafine particles (UFPs, Dp < 100 nm) are ubiquitous in the urban environment (Kumar et al., 2014), and are of concern owing to their adverse effects on human health (Araujo et al., 2008; Atkinson et al., 2010). UFPs vary from larger sized ambient particles in their potential for lung deposition and translocation to other parts of the body (HEI, 2013). Previous studies have shown that UFPs easily penetrate the respiratory system and transfer to the extra-pulmonary organs such as the central nervous system (Elder et al., 2006; Elder and Oberdörster, 2006; Oberdorster et al., 2004).

Sources of UFPs in the urban atmosphere include primary emissions - from motor vehicles, coal-fired power plants, gas-fired facilities, and biomass burning in winter (Kumar et al., 2014; Morawska et al., 2008; Wehner et al., 2009; Zhu et al., 2002), and those formed as new particles via nucleation (Brock et al., 2002; Holmes, 2007; Kulmala and Kerminen, 2008). The major source of primary UFPs in urban areas is combustion, with previous studies demonstrating that UFP particle numbers correlate with the local traffic activity, in particular in the morning and afternoon rush hours (Alam et al., 2003; Harrison and Jones, 2005). These particles can be produced in the engine or in the ambient air after emission from the vehicle tailpipe (Charron and Harrison, 2003; Shi et al., 1999). Primary UFPs associated with traffic are released during the dilution and cooling of vehicle exhaust (Charron and Harrison, 2003; Kittelson et al., 2006) or formed by fuel combustion as, for example, carbonaceous soot (Kittelson, 1998; Shi et al., 2000).

Previous studies found that total particle number consists of 80-90% UFPs (Mejia et al., 2008; Rodríguez et al., 2007; Wehner and Wiedensohler, 2003). Reche et al. (2011) have shown from the characterisation of total particle number concentrations in various European urban background sites that total particle number is a good representation of the UFPs in an urban area.

Previous studies measuring UFPs in urban areas have measured particles larger than 7 nm (Harrison and Jones, 2005; Shi et al., 2001) and 3 nm (Shi et al., 1999). Many studies have indicated that the two main sources of UFPs in urban areas (Brines et al., 2015; Dunn et al., 2004; Morawska et al., 2008; Reche et al., 2011; Rodríguez and Cuevas, 2007) are:

- *Vehicle exhausts emissions*. These particles tend to exhibit bimodal size distribution, with a nucleation (<20 nm) and a carbonaceous mode (50-200 nm). The nucleation mode (<20 nm) particles are not produced directly from vehicle exhaust emissions, but

are created through nucleation (gas-to-particle conversion). In urban areas this occurs after rapid cooling and dilution of exhaust emissions when the saturation ratio of gaseous mixtures of low volatility (i.e. sulphuric acid) reaches a maximum (Arnold et al., 2006; Burtscher, 2005; Charron and Harrison, 2003; Kittelson et al., 2006). The carbonaceous mode (50-200 nm) is mainly composed of soot (Casati et al., 2007; Rose et al., 2006).

New particle formation in ambient air. This process may be caused by the photochemical reactions of naturally emitted gaseous precursors in ambient air by "*in-situ* nucleation" happening after emission. This mechanism includes two main steps, with nucleation of an initial cluster (<1 nm) and the initiation of such cluster resulting in particle growth (Kulmala et al., 2004). It is considered that the nucleation of sulfuric acid gas molecules play a significant role in the formation of such stable clusters, and may also contribute in particle growth by condensation (Kulmala et al., 2006). Recent studies have shown that ammonium and highly oxidised organic molecules may also play an important role in nucleation (Ehn et al., 2014; Kirkby et al., 2011).

A number of studies have reported quantifying the sources and processes that contribute to UFP in urban areas (Fernández-Camacho et al., 2010; González and Rodríguez, 2013; González et al., 2011; Kulmala et al., 2016; Reche et al., 2011; Rodríguez and Cuevas, 2007). However, no studies to date have reported the quantification of the sources and processes that contribute to UFP in UK cities. In this context, the main aim of this paper is to study the factors responsible for the variability of TNC, eBC, and the gaseous pollutants at a UK urban background site in Leicester. A specific focus of the work is the relative contributions of primary and secondary sources to the observed total particle number concentrations. To our knowledge, this study represents the first that explores the variability of TNC and its sources in the UK urban background.

The study was carried out between January 2014 and December 2015 over which time TNC was measured concurrently with eBC, nitrogen oxides concentration (NO_X) and particle number size distributions (PNSD) at the AURN (Automatic Urban and Rural Network) site in Leicester (UK). This study was carried out as part of the JOint Air QUality INitiative (JOAQUIN, www.joaquin.eu), an INTERREG IVB funded European project, aimed at supporting health-oriented air quality policies in Europe (Cordell et al., 2016; Hama et al., 2017b; Hama et al., 2017a; Hofman et al., 2016).

2. Methods

2.1 Measurement site

Measurements were carried out at the University of Leicester urban background site (lat 52°37′11.36″ N, long 1°07′38.32″ W) a permanent site which is part of both JOAQUIN UFP NWE observatory system and the national Defra Automatic Urban Rural Network (AURN). The site is located on the University of Leicester campus (http://uk air.defra.gov.uk/networks/site-info?uka_id=UKA00573) and is shown in Figure 1. The nearest road is University Road (20 m north-west) and the nearest main road is Welford Road (140 m south-south west). According to traffic counts by the Department for Transport, the traffic intensity on the Welford Road was about 22600 vehicles/day in 2014 (http://www.dft.gov.uk/traffic-counts, count point 36549). For a detailed overview of the monitoring sites and the JOAQUIN project, the reader is referred to the final report (Joaquin, 2015).

2.2 Instrumentation

Table 1 summarizes the availability of monitors for PNC, TNC, eBC, PM2.5 and the gaseous pollutants at the AURN site. Size-resolved particle number concentrations (PNC; # cm^{-3}) were obtained using UFP Monitor (UFPM, TSI 3031). PNC were quantified in six size classes (20-30, 30-50, 50-70, 70-100, 100-200 and > 200 nm), using an UFPM (see Table 1). For this study five channels (20-30, 30-50, 50-70, 70-100, 100-200 nm) were used and the size class (>200 nm) was ignored owing to low number concentrations (Joaquin, 2015). The UFP monitor's operation is based on electrical diffusion charging of the particles, size segregation by means of a DMA, followed by aerosol detection using a Faraday cup electrometer (Hofman et al., 2016; Joaquin, 2015). The performance of this instrument has been explored against other UFP measurement system in Hofman et al. (2016). The TNC was measured by a Water-Based Condensation Particle Counter (W-CPC, TSI Environmental Particle Counter (EPC) model 3783 http://www.tsi.com/environmental-particle-counter-3783).

The TSI instruments (UFP monitor and W-CPC) were connected to an environmental sampling system (TSI 3031200). The components of the TSI 3031200 are a PM_{10} inlet, sharp cut PM_1 cyclone, flow splitter and Nafion dryer (reduces humidity to less than 50% RH).

The mass concentration of equivalent black carbon (eBC) was measured by a Multi-angle Absorption Photometer (MAAP Thermo Scientific model 5012) for the whole period (Petzold et al., 2013). The MAAP determines particle light absorption due to the light transmission and backscattering at two angles of particles collected on the filter tape (glass fibre type GF10). The eBC mass concentration is calculated using a constant mass absorption cross section of 6.6 g/m^2.

Nitrogen oxides were also measured by a Thermo 42i NO-NO_2-NO_x monitor. This monitor uses chemiluminescence technology to measure the concentration of nitrogen oxides in the air. It has a single chamber, single photomultiplier tube design that cycles between the NO and NO_x mode.

Meteorological data (temperature, relative humidity, solar radiation and wind speed and direction) were provided for 2014 by the Air Quality Group from the Leicester City Council. The station is located 4.9 km away from the AURN urban background monitoring site, and the meteorological data for 2015 were measured at the AURN site.

2.3 Data processing and analysis

The raw 10 min-data were validated by screening for irregularities and removing data collected during instrument errors and maintenance periods. All validated data were subsequently aggregated to 30 min intervals. Data analyses have been carried out using the Open-air software package (Carslaw, 2015; Carslaw and Ropkins, 2012) using R software (R Core Team, 2015).

3. Results and discussion

3.1 Annual Variation

Monthly particle TNC and PNC (five size classes), and other air quality parameters, such as eBC, NOx, $PM_{2.5}$, O_3, and CO are shown in Figure 2 and Figure S1**.** Figure 2 shows that higher values of TNC and PNC (except small sizes, 20-30 nm) were found in the cooler months. The TNC profiles show a peak in winter (November to January), which might be associated with factors such as an increase in wood burning for domestic heating (Cordell et al., 2016), reduced dispersion of local sources and a low mixing height in winter. In addition, TNC shows two peaks, one in March and the other in June (see Figure 2). This could be related to NPF since previous studies have demonstrated that NPF occurs in spring and summer at this site (Hama et al., 2017b; Hofman et al., 2016). However, PNC (100-200nm) concentrations were observed to be highest in winter and lowest in summer. The observed seasonal cycle can be linked to the previously detailed reasons as well as metrological factors (dilution effect, (see Hama et al., 2017a)) that have a significant impact in seasonal variations. For example, UFP will be influenced by the temperature dependent volatility of the traffic-generated particles which produces high particle number concentrations during the cold period (Bigi and Harrison, 2010; Charron and Harrison, 2003; Hofman et al., 2016; Mishra et al., 2012) coupled to cold period boundary layer stability. Interestingly, high concentrations of PNC (small sizes, 20-30 nm) were found during the spring and summer months. In particular, this is clear for the small particles (20-30 nm) (see Figure 2). The observed increase in spring may be related to NPF which has been observed at this site (Hama et al., 2017b; Hama et al., 2017a; Hofman et al., 2016)**.**

A summary of the pollutant concentrations at AURN site are given in Table S1. TNC and eBC concentrations observed were comparable to levels found in other European urban background sites (Hofman et al., 2016; Keuken et al., 2015; Reche et al., 2011). The mean annual TNC and eBC concentration were 8022 # cm^{-3} and 1.45 μg m^{-3}, with a standard deviation of 5514 # cm^{-3} and 1.39 μg $m^{-3,}$ respectively. The annual average PNC for the five size classes were: i) 1457 # cm^{-3} (20-30 nm), ii) 1704 # cm^{-3} (30-50 nm), iii) 1193 # cm^{-3} (50-70 nm), iv) 1059 # cm^{-3} (70-100 nm), v) 980 # cm^{-3} (100-200 nm). According to these results it can be concluded that ultrafine particles (particles < 100 nm) were the dominant particle size range. The annual average levels of the other pollutants as shown in Table S1 are comparable to concentrations reported in other European urban areas (Hofman et al., 2016; Pérez et al., 2010 and references

therein; Reche et al., 2011). The annual patterns of NOx, CO, eBC, and $PM_{2.5}$ are comparable to one another, with the highest levels occurring in the cold season and the lowest in summer (see Figure S1). The cold period average concentrations were larger by a factor of 1.5, 1.3, 1.35, and 1.3 with respect to the warm mean value for NOx, CO, eBC, and $PM_{2.5}$, respectively. The highest levels of these constituents in the cold season are attributable to emissions from a variety of sources including traffic and an increase in domestic heating, for example from wood burning as reported in recent study at this site (Cordell et al., 2016), coupled to reduced dispersion (Harrison et al., 2012). The annual variations are also modulated by the annual variations in meteorological, dynamic and synoptic conditions (Barmpadimos et al., 2012; Bigi and Harrison, 2010; Reche et al., 2011; Ripoll et al., 2014). As would be expected, the O_3 annual variation shows a minimum in October and November and a maximum in spring, especially in May (Monks, 2000). The low O_3 levels in autumn and winter are related to lower temperatures, less solar radiation, and also the chemical titration reaction with NO from the higher emissions of NOx associated with domestic heating in autumn and winter months leading to a decrease in O_3, as observed in other studies (Lin et al., 2011; Lin et al., 2008).

Finally, it is clear that the measured TNC and PNC (particularly small particles, 20-30nm) in cold period were similar to warm period (1.1 and 1.01 for TNC, and $PNC_{20\text{-}30nm}$). It can be concluded that domestic heating and metrological conditions in cold months and NPF in the warm period have the greatest impact on seasonal variations of particle number concentrations in Leicester.

3.2 Weekly and Daily variations

The weekly cycle of TNC and PNC for 2014 at the AURN site are shown in Figure 3 and TNC for 2015 is shown in Figure S2. TNC average concentrations were slightly lower at the weekend (7500 # cm^{-3}), than working days (8400 # cm^{-3}) (see Figure 3), indicating that the pollutant levels were influenced not only by anthropogenic emissions (such as traffic emissions), but also could be associated with local or regional non-anthropogenic origin sources. Moreover, PNC size range concentrations showed a weekly cycle (see Figure 3), with the lowest average levels occurring during weekends and the highest on weekdays, especially on Mondays. The average concentrations of $PNC_{20\text{-}30}$, $PNC_{30\text{-}50}$, $PNC_{50\text{-}70}$, $PNC_{70\text{-}100}$, and $PNC_{100\text{-}200}$ for working days are 1516, 1738, 1206, 1068, and 986 # cm^{-3} and for weekends are 1363, 1664, 1143, 1017, 922 # cm^{-3}, respectively. eBC also showed the highest mean values

(1.41 μg m^{-3}) on working days (see Figure S2), and lower concentrations (1.1 μg m^{-3}) during weekends. This is probably related to decreased traffic emissions during weekends. The weekly cycle of gaseous pollutants (NO, NO_2, NOx, CO, O_3), and $PM_{2.5}$, concentrations at AURN site are shown in Figure S2 **.** All pollutants, except ozone, showed a similar pattern with a minimum at weekends, especially on Sundays. However, on Sundays O_3 concentrations peaked, due to the so-called O_3 weekend effect (Larsen et al., 2003). The observed behaviour is consistent with previous studies (Bigi and Harrison, 2010; Pérez et al., 2010; Ripoll et al., 2014; Yoo et al., 2015).

The eBC diurnal patterns are shown in Figure 4. eBC shows the same profile as the traffic-related gaseous pollutants in the morning owing to the morning rush hour (high traffic, low wind speed), but conversely to the gaseous pattern, the eBC concentrations decreased sharply after the morning rush hour until increasing again during evening rush hour. This might be associated to decreased traffic volume, increased wind speed (high dilution at midday), and increased mixing height. Similar results were found in other European urban background sites (Annual Report for the UK Black Carbon Network, 2014; Dall'Osto et al., 2013; Hofman et al., 2016; Pérez et al., 2010; Reche et al., 2011; Rodríguez et al., 2008). The variation of the eBC in warmer months (May-Sep), however, shows a weaker diurnal pattern, with a stronger diurnal variation being observed during the cold period most likely caused by the synoptic condition, and may relate to the larger domestic heating emissions during the evening (Allan et al., 2010; Cordell et al., 2016) coupled to greater atmospheric stability.

The daily variation of TNC was similar to that of eBC, suggesting it is also highly influenced by traffic emissions. The profiles matched well during the cold period, however, during the summer season the TNC peaks, showing especially a second peak that corresponds to the evening rush hour. This rush hour peak became less obvious or later in the colder months. These observations can be explained by comparison to the patterns observed in eBC concentration: during the night the TNC decreased owing to the low traffic volumes, which when combined with the decrease of the boundary layer height, favours lower ultrafine particles numbers owing to the condensation and coagulation processes (Minoura and Takekawa, 2005; Pérez et al., 2010). Interestingly, during the warm period another TNC peak was observed at noon (see Figure 4) which did not follow the eBC pattern. It can be concluded that the TNC peak cannot be from primary particle emissions from traffic. This extra TNC peak can be attributed to NPF resulting from photochemical nucleation reactions from gaseous precursors (Hama et al., 2017b; Hofman et al., 2016). The observed midday peak coincides

with higher solar radiation, an increase in wind speed (not shown) and the growth of the mixing layer (Rodríguez et al., 2007). The detail of primary and secondary sources of TNC will be discussed in the section 3.3 and 3.4**.**

The daily cycle of PNC (five size bins) showed a similar variation to the traffic related pollutants such as eBC and TNC as shown in Figure 5. During the cold period, the diurnal variation of PNC (mostly UFPs) had two peaks which followed the morning and afternoon traffic rush hours. However, like the other parameters measured during warm period the daily cycle was weaker and the evening peak was not clearly observed. There is a notable difference in the diurnal cycles of $PNC_{20\text{-}30}$ (red line) during the warm season. $PNC_{20\text{-}30}$ shows another peak at midday, as recorded for the TNC. Those particles can be attributed as the small particles from NPF (Hama et al., 2017b).

Levels of the gaseous pollutants (NO, NO_2, NOx, O_3), monitored at the AURN site were predominantly influenced by vehicle traffic emission, evolution of the mixing layer, and meteorological conditions. Figure S3 shows the diurnal patterns of the atmospheric gaseous pollutants (NO, NO_2, NOx, and O_3) for the year 2015. It can be seen all the gaseous pollutant peaks (except O_3) followed the diurnal variation of vehicular traffic emissions, with increasing levels of the gaseous pollutants measured in the morning rush hour (high traffic intensity, poor dispersion), which then decreased during the day, owing to atmospheric dilution effects, before increasing once more in the evening rush hour. Finally, it can be concluded that particle number concentrations are influenced by primary and secondary sources in Leicester (see Section 3.3 for more detail).

3.3 Exploring the Relationship between total particle number and black carbon concentrations

Traffic emissions in the urban environment in Europe tend to drive the correlation between TNC and eBC (Fernández-Camacho et al., 2010; Pérez et al., 2010; Reche et al., 2011; Rodríguez and Cuevas, 2007; Rodríguez et al., 2007). The correlation between TNC and eBC has been analysed at the Leicester AURN site using the methodology described by Rodríguez and Cuevas (2007). The correlation between TNC and eBC for four different time periods of the day (07:00-09:00, 11:00-14:00, 17:00-20:00, and 00:00-04:00) is shown in Figure 6. The selection of these time ranges are based upon the diurnal variations of TNC and eBC, which are mostly governed by traffic emissions and atmospheric dynamics in the Leicester urban

environment. At any time of the day, the TNC versus eBC scatter plots clearly showed two defined linear cut-offs with slopes S1 and S2, representing the minimum and maximum TNC/eBC ratios, respectively (see Figure 6). S1 represents the minimum TNC/eBC ratio, which is interpreted as representative of the primary particles, mostly from vehicle exhaust emissions. S2 is the maximum TNC/eBC ratio (see Figure S4), which is interpreted as arising predominately from secondary particles, mainly from NPF during the dilution and cooling of the vehicle exhaust emissions in the urban environment (Rodríguez and Cuevas, 2007). Table 2 shows the values of slopes S1 and S2 found at different times of the day. During the morning rush hours (07:00-09:00), when the NOx peaks, owing to vehicle exhaust emissions, values of S1= 2.53×10^6 particles /ng eBC, and S2= 2.85×10^6 particles /ng eBC were obtained. The S1value found at the AURN site (see Table 3) was higher than values found in Hyytiälä and Nanjing. It is comparable to values found in some cities (London, Lugano, and Bern). However, the S1 value is lower than values obtained in Milan, Huelva, Santa Cruz de Tenerife, and Barcelona (see Table 3). It should be noted that the greater values of S1 in earlier studies were influenced by the selection of the CPC model used, as the higher the cut size of the CPC monitor the lower the N/BC ratio (Reche et al., 2011). Another variable is the distance of the sites from fresh traffic emissions. In addition, the size of the eBC cores might be smaller than that from regular from traffic emissions. This behaviour is observed when points occur below the line S1 as shown in Figure 6. The size of eBC is generally smaller from fresh traffic emissions compared with that from other primary particle sources (Bond et al., 2013). A small size of the eBC core in primary particle sources is likely to increase the S1 value (Kulmala et al., 2016). The diameter of eBC core can be found by application of Eq.1 assuming that the core is spherical:

$$D_P = \left[{}^{6}/_{(\pi S1\rho)}\right]^{1/3} \qquad (1)$$

Where $\boldsymbol{\rho}$ is the core density. The density of non-volatile components of diesel soot is about 1.7-1.8 gcm^{-3} (Park et al., 2004, Zhang et al., 2008). By using the core density and the value of S1 (07:00-09:00) in Table 2, the diameter of the eBC core was found to be in the range of 75-96 nm at the AURN site. This result indicates that eBC and UFP are co-emitted by the vehicle fleet and they show a high degree of correlation. This shows that eBC and UFP are externally

well mixed at this site in Leicester. This result is consistent with the general knowledge regarding eBC particle size at urban background sites (Schwarz et al., 2008). Finally, it can be concluded that the value of S1 may depend on the size of the eBC emitted by vehicular exhaust during this study at AURN site.

3.4 Segregating the components contributing to UFPs

By using the methodology described by Rodríguez and Cuevas (2007), the TNC measured at AURN site was segregated into two components, in order to identify the sources and processes influencing the particle number concentrations.

$$\mathrm{N1} = \mathrm{S1.eBC} \qquad (2)$$

$$\mathrm{N2} = \mathrm{TNC} - \mathrm{N1} \qquad (3)$$

Where, S1= 2.53×10^{6} particles/ng eBC (see Table 2). N1 is the minimum primary emission of vehicle exhaust which includes "those components directly emitted in the particle phase" and "those compounds nucleating immediately after the vehicle exhaust emission" (Rodríguez and Cuevas, 2007). Component N2 represents the secondary particles formed in ambient air by nucleation, impact of atmosphere conditions on the ultrafine particle formation during the dilution and cooling of the vehicle exhaust emissions and other sources different from vehicle exhaust which contribute to TNC.

These interpretations of source function are supported by the data as shown in Figure 7 and Figure 8**.** Figure 7 shows half-hourly average values of N1 and N2 with NOx, O_3 and wind speed for every day of the week. The weekly evolution of N1 and N2 present two different patterns (Figure 7a). The N1 profile follows the NOx profile, with the maximum percentage of N1 during morning and evening rush hours on working days, when ultrafine particles are mainly associated with vehicle exhaust emissions, 49%, and 46%, respectively (Figure 7b and Table 4). However, the N2 pattern follows the O_3 daily evolution and wind speed (Figure 7c, with the maximum at midday (N2= 62%, Table 4). The daily pattern of N2 is significantly different from that of N1, as shown in Figure 7a, and also from the $PM_{2.5}$ diurnal variation (see

Figure S5). This behaviour of N2 might be linked to the NPF events at midday at AURN site (Hama et al., 2017b; Hofman et al., 2016). Moreover, the similar pattern of N2 and temperature (Figure 8a) may suggest an active role for the oxidation products of any VOCs. Furthermore, Figure 8b shows an inverse correlation between N2 and RH which supports that the NPF processes at midday occur at a lower RH. Generally, the percentage of N2 (57%) was greater than the percentage of N1 (43%) for all days at the AURN site for the whole study. The high percentage of N2 could be related to the primary sources from non-traffic emissions such as domestic heating (Cordell et al., 2016) and resuspension and biogenic and VOCs emissions in Leicester. Previous studies have reported that the high N2 is caused by the combination of high solar radiation and dilution of pollutants when the boundary layer increases, as well as SO_2 concentrations (not measured at AURN site) (Reche et al., 2011). Overall, this study demonstrated that secondary particle formation is the main contributor to particle number concentration in Leicester.

3.5 Dependency on wind speed and direction

The relationship between traffic-related pollutants (TNC, eBC, NOx) and wind conditions is shown in Figure 9(a-f). The plots show that concentrations of the three parameters were dominated by north and south-westerly wind directions. The bivariate polar plots (Figure 9a, c, and e) show how the parameters varied by wind direction and speed at AURN site. These plots are very useful for identifying and determining sources and direction of the pollutants (Carslaw and Ropkins, 2012). For TNC, Figure 9a shows that there is evidence of increasing TNC when the wind speed increases from the west, north-west, and south-west. Higher TNC was found at low wind speed (<2 m s^{-1}) owing to local sources, mainly traffic emissions. In addition, at high wind speed (5-10 m s^{-1}) high TNC was also found mostly from the north-west which indicates a potential contributor to TNC that may be East Midlands Airport (located *ca.* 27 km north-west of AURN site). This behaviour has been observed in other European studies (Hofman et al., 2016; Keuken et al., 2015). In the case of eBC, Figure 9c shows a similar pattern to TNC. The prevailing wind directions were from the north and north-west. The major eBC contribution came from these N-NW directions independent of wind speed. In addition, high eBC concentrations where categorised at high wind speed (10-12 m s^{-1}) when the wind was blowing from the north-east. For NOx, Figure 9e shows that the highest concentrations are associated with winds from north-west and south-west, at lower speeds (<2 m s^{-1}) and also

at higher wind speeds (4-8 m s^{-1}). The most probable source of NOx is the vehicle exhaust emissions at this site. The highest concentrations of TNC, eBC, and NOx were observed with north and south-westerly winds and were mostly associated with the lower wind speeds (< 10m s^{-1}). These observations support the outlook that urban background of these pollutant concentrations is dominated by local sources, rather than regional sources. The polar annulus plots for TNC, eBC, and NOx are presented in Figure 9b, d and f, respectively**.** The patterns for the three parameters are consistent with a main traffic contribution from the nearby roads (University Road and Welford Road), with the maximum concentrations occurring during morning and evening rush hours. These roads are located at around 50-140 m to the north and south west of AURN site (see section 2.1). Moreover, it is interesting to note that in Figure 9b (for TNC) the highest concentrations occurred around noon linked to the NPF at AURN site (described in detail in section 3.1). To confirm this behaviour, the relationship between N1 and N2 and wind conditions are presented in Figure 10 (a-b). Figure 10a shows the highest N1 concentrations occur with winds from north-west. In addition, it can be seen high N2 concentrations of N1 are observed during morning and evening rush hours (see Figure 10b). This behaviour indicates that N1 is affected by primary sources such as traffic emissions. In the case of N2 (Figure 10c and d) a different pattern in terms of wind direction and time of the day is observed: high N2 concentrations were found with the wind blowing from the south-west (see Figure 10c). Interestingly, Figure 10d shows high N2 concentrations occuring around noon, correlating with the behaviour of TNC **(**Figure 9b**)** and could be related to NPF events at the AURN site. Lastly, it can be concluded that wind conditions have a significant impact on N1, and N2 at the AURN site. Furthermore, the effect of differing wind conditions on N1 and N2 also revealed that they are influenced by different sources in the Leicester urban area.

The relationships between the TNC, eBC, and NOx with wind speed have also been analysed (not shown) and show that the highest concentrations of the parameters are observed at low wind speed (< 5 m s^{-1}). This is a typical behaviour of urban background site and is comparable with other European studies (Charron and Harrison, 2003; Pérez et al., 2010; Voigtländer et al., 2006; von Bismarck-Osten et al., 2013; Weber et al., 2013; Wehner and Wiedensohler, 2003).

4. Conclusions

This study shows the results of long-term measurements (2014-2015) and interpretation of the variability of TNC, PNC, $PM_{2.5}$, eBC, and the gaseous pollutants at the AURN urban background site in Leicester. The results demonstrate that the temporal variations of TNC are not always solely caused by road traffic emissions, whereas eBC concentrations closely follow other road traffic related pollutants, such as NOx. The contributions of primary and secondary particle sources to the TNC were identified using the eBC concentration as a tracer for primary particles. By using the minimum slope found in the TNC versus eBC plot (2.53×10^6 particles/ng eBC), TNC was segregated into two components, TNC = N1 + N2. The highest N1 (49%) were recorded during the morning rush hours (07:00-09:00 h), when maximum NOx levels were recorded. Component N2 shows a profile well differentiated from that of N1 and is associated to those processes leading to increase the TNC/BC ratio, i.e. enhancement in NPF rates owing to increased nucleation and/or growth rates to limit sizes (≥ 7 nm in our case). The maximum contribution of N2 to TNC was found around midday (11:00-14:00), where it was about 62%, when low eBC and high O_3 levels were recorded. Moreover, the majority of particles were expected to be of secondary origin. The impact of wind speed and direction also show different sources of N1 and N2. According to the bivariate polar plots, high N2 concentrations were found around noon. Finally, this long-term study has shown that primary and secondary sources of UFPs at one urban background site in UK.

Acknowledgements

The authors would like to thank the Human Capacity Development Program from the Kurdistan Government for a scholarship (S.M.L.HAMA). We would like to thank Dr.Sergio Rodríguez to his help and suggestions. We would like also to thank Dr Jolanta Obszynska (Leicester City Council) for providing meteorological data. This research was funded by the Joint Air Quality Initiative (JOAQUIN) project, part of the EU Interreg IV-B NWE Program.

References

Alam, A., Shi, J.P., Harrison, R.M., 2003. Observations of new particle formation in urban air. Journal of Geophysical Research: Atmospheres 108, n/a-n/a.

Allan, J.D., Williams, P.I., Morgan, W.T., Martin, C.L., Flynn, M.J., Lee, J., Nemitz, E., Phillips, G.J., Gallagher, M.W., Coe, H., 2010. Contributions from transport, solid fuel burning and cooking to primary organic aerosols in two UK cities. Atmos. Chem. Phys. 10, 647-668.

Annual Report for the UK Black Carbon Network, 2014. 2014 Annual Report for the UK Black Carbon Network, National Physical Laboratory, Hampton Road, Teddington, Middlesex, TW11 0LW.

Araujo, J.A., Barajas, B., Kleinman, M., Wang, X., Bennett, B.J., Gong, K.W., Navab, M., Harkema, J., Sioutas, C., Lusis, A.J., Nel, A.E., 2008. Ambient particulate pollutants in the ultrafine range promote early atherosclerosis and systemic oxidative stress. Circulation research 102, 589-596.

Arnold, F., Pirjola, L., Aufmhoff, H., Schuck, T., Lahde, T., Hameri, K., 2006. First gaseous sulfuric acid measurements in automobile exhaust: Implications for volatile nanoparticle formation. Atmospheric Environment 40, 7097-7105.

Atkinson, R.W., Fuller, G.W., Anderson, H.R., Harrison, R.M., Armstrong, B., 2010. Urban ambient particle metrics and health: a time-series analysis. Epidemiology 21, 501-511.

Barmpadimos, I., Keller, J., Oderbolz, D., Hueglin, C., Prévôt, A.S.H., 2012. One decade of parallel fine (PM_{2.5}) and coarse (PM₁₀–PM_{2.5}) particulate matter measurements in Europe: trends and variability. Atmospheric Chemistry and Physics 12, 3189-3203.

Bigi, A., Harrison, R.M., 2010. Analysis of the air pollution climate at a central urban background site. Atmospheric Environment 44, 2004-2012.

Bond, T.C., Doherty, S.J., Fahey, D.W., Forster, P.M., Berntsen, T., DeAngelo, B.J., Flanner, M.G., Ghan, S., Kärcher, B., Koch, D., Kinne, S., Kondo, Y., Quinn, P.K., Sarofim, M.C., Schultz, M.G., Schulz, M., Venkataraman, C., Zhang, H., Zhang, S., Bellouin, N., Guttikunda, S.K., Hopke, P.K., Jacobson, M.Z., Kaiser, J.W., Klimont, Z., Lohmann, U., Schwarz, J.P., Shindell, D., Storelvmo, T., Warren, S.G., Zender, C.S., 2013. Bounding the role of black carbon in the climate system: A scientific assessment. Journal of Geophysical Research: Atmospheres 118, 5380-5552.

Brines, M., Dall'Osto, M., Beddows, D.C.S., Harrison, R.M., Gómez-Moreno, F., Núñez, L., Artíñano, B., Costabile, F., Gobbi, G.P., Salimi, F., Morawska, L., Sioutas, C., Querol, X., 2015. Traffic and nucleation events as main sources of ultrafine particles in high-insolation developed world cities. Atmospheric Chemistry and Physics 15, 5929-5945.

Brock, C.A., Washenfelder, R.A., Trainer, M., Ryerson, T.B., Wilson, J.C., Reeves, J.M., Huey, L.G., Holloway, J.S., Parrish, D.D., Hubler, G., and Fehsenfeld, Fred C. , 2002. Particle growth in the plumes of coal-fired power plants. Journal of Geophysical Research 107.

Burtscher, H., 2005. Physical characterization of particulate emissions from diesel engines: a review. Journal of Aerosol Science 36, 896-932.

Carslaw, D.C., 2015. The openair manual — open-source tools for analysing air pollution data. King's College London.

Carslaw, D.C., Ropkins, K., 2012. openair — An R package for air quality data analysis. Environmental Modelling & Software 27-28, 52-61.

Casati, R., Scheer, V., Vogt, R., Benter, T., 2007. Measurement of nucleation and soot mode particle emission from a diesel passenger car in real world and laboratory in situ dilution. Atmospheric Environment 41, 2125-2135.

Charron, A., Harrison, R.M., 2003. Primary particle formation from vehicle emissions during exhaust dilution in the roadside atmosphere. Atmospheric Environment 37, 4109-4119.

Cordell, R.L., Mazet, M., Dechoux, C., Hama, S.M.L., Staelens, J., Hofman, J., Stroobants, C., Roekens, E., Kos, G.P.A., Weijers, E.P., Frumau, K.F.A., Panteliadis, P., Delaunay, T., Wyche, K.P., Monks, P.S., 2016. Evaluation of biomass burning across North West Europe and its impact on air quality. Atmospheric Environment 141, 276-286.

Dall'Osto, M., Querol, X., Alastuey, A., O'Dowd, C., Harrison, R.M., Wenger, J., Gómez-Moreno, F.J., 2013. On the spatial distribution and evolution of ultrafine particles in Barcelona. Atmospheric Chemistry and Physics 13, 741-759.

Dunn, M.J., Jiménez, J.-L., Baumgardner, D., Castro, T., McMurry, P.H., Smith, J.N., 2004. Measurements of Mexico City nanoparticle size distributions: Observations of new particle formation and growth. Geophysical Research Letters 31, n/a-n/a.

Ehn, M., Thornton, J.A., Kleist, E., Sipila, M., Junninen, H., Pullinen, I., Springer, M., Rubach, F., Tillmann, R., Lee, B., Lopez-Hilfiker, F., Andres, S., Acir, I.H., Rissanen, M., Jokinen, T., Schobesberger, S., Kangasluoma, J., Kontkanen, J., Nieminen, T., Kurten, T., Nielsen, L.B., Jorgensen, S., Kjaergaard, H.G., Canagaratna, M., Maso, M.D., Berndt, T., Petaja, T., Wahner, A., Kerminen, V.M., Kulmala, M., Worsnop, D.R., Wildt, J., Mentel, T.F., 2014. A large source of low-volatility secondary organic aerosol. Nature 506, 476-479.

Elder, A., Gelein, R., Silva, V., Feikert, T., Opanashuk, L., Carter, J., Potter, R., Maynard, A., Ito, Y., Finkelstein, J., Oberdörster, G., 2006. Translocation of Inhaled Ultrafine Manganese Oxide Particles to the Central Nervous System. Environmental Health Perspectives 114, 1172-1178.

Elder, A., Oberdörster, G., 2006. Translocation and effects of ultrafine particles outside of the lung. Clin Occup Environ Med. 4, 785-796.

Fernández-Camacho, R., Rodríguez, S., de la Rosa, J., Sánchez de la Campa, A.M., Viana, M., Alastuey, A., Querol, X., 2010. Ultrafine particle formation in the inland sea breeze airflow in Southwest Europe. Atmospheric Chemistry and Physics 10, 9615-9630.

González, Y., Rodríguez, S., 2013. A comparative study on the ultrafine particle episodes induced by vehicle exhaust: A crude oil refinery and ship emissions. Atmospheric Research 120-121, 43-54.

González, Y., Rodríguez, S., Guerra García, J.C., Trujillo, J.L., García, R., 2011. Ultrafine particles pollution in urban coastal air due to ship emissions. Atmospheric Environment 45, 4907-4914.

Hama, S.M.L., Cordell, R.L., Kos, G.P.A., Weijers, E.P., Monks, P.S., 2017b. Sub-micron particle number size distribution characteristics at two urban locations in Leicester. Atmospheric Research 194, 1-16.

Hama, S.M.L., Ma, N., Cordell, R.L., Kos, G.P.A., Wiedensohler, A., Monks, P.S., 2017a. Lung deposited surface area in Leicester urban background site/UK: Sources and contribution of new particle formation. Atmospheric Environment 151, 94-107.

Harrison, R.M., Jones, A.M., 2005. Multisite Study of Particle Number Concentrations in Urban Air. Environ. Sci. Technol 39, 6063-6070.

Harrison, R.M., Laxen, D., Moorcroft, S., Laxen, K., 2012. Processes affecting concentrations of fine particulate matter (PM2.5) in the UK atmosphere. Atmospheric Environment 46, 115-124.

HEI, 2013. HEI Review Panel on Ultrafine Particles. Understanding the Health Effects of Ambient Ultrafine Particles, HEI Perspectives 3., Health Effects Institute, Boston, MA.

Hofman, J., Staelens, J., Cordell, R., Stroobants, C., Zikova, N., Hama, S.M.L., Wyche, K.P., Kos, G.P.A., Van Der Zee, S., Smallbone, K.L., Weijers, E.P., Monks, P.S., Roekens, E., 2016. Ultrafine particles in four European urban environments: Results from a new continuous long-term monitoring network. Atmospheric Environment 136, 68-81.

Holmes, N.S., 2007. A review of particle formation events and growth in the atmosphere in the various environments and discussion of mechanistic implications. Atmospheric Environment 41, 2183-2201.

Joaquin, 2015. Monitoring of ultrafine particles and black carbon. Joint Air Quality Initiative, Work Package 1 Action 1 and 3, Flanders Environment Agency, Aalst. Available at http://www.joaquin.eu.

Keuken, M.P., Moerman, M., Zandveld, P., Henzing, J.S., Hoek, G., 2015. Total and size-resolved particle number and black carbon concentrations in urban areas near Schiphol airport (the Netherlands). Atmospheric Environment 104, 132-142.

Kirkby, J., Curtius, J., Almeida, J., Dunne, E., Duplissy, J., Ehrhart, S., Franchin, A., Gagne, S., Ickes, L., Kurten, A., Kupc, A., Metzger, A., Riccobono, F., Rondo, L., Schobesberger, S., Tsagkogeorgas, G., Wimmer, D., Amorim, A., Bianchi, F., Breitenlechner, M., David, A., Dommen, J., Downard, A., Ehn, M., Flagan, R.C., Haider, S., Hansel, A., Hauser, D., Jud, W., Junninen, H., Kreissl, F., Kvashin, A., Laaksonen, A., Lehtipalo, K., Lima, J., Lovejoy, E.R., Makhmutov, V., Mathot, S., Mikkila, J., Minginette, P., Mogo, S., Nieminen, T., Onnela, A., Pereira, P., Petaja, T., Schnitzhofer, R., Seinfeld, J.H., Sipila, M., Stozhkov, Y., Stratmann, F., Tome, A., Vanhanen, J., Viisanen, Y., Vrtala, A., Wagner, P.E., Walther, H., Weingartner, E., Wex, H., Winkler, P.M., Carslaw, K.S., Worsnop, D.R., Baltensperger, U., Kulmala, M., 2011. Role of sulphuric acid, ammonia and galactic cosmic rays in atmospheric aerosol nucleation. Nature 476, 429-433.

Kittelson, D.B., 1998. ENGINES AND NANOPARTICLES: A REVIEW. J. Aerosol Sci. 29, 575-588.

Kittelson, D.B., Watts, W.F., Johnson, J.P., 2006. On-road and laboratory evaluation of combustion aerosols—Part1: Summary of diesel engine results. Journal of Aerosol Science 37, 913-930.

Kulmala, M., Kerminen, V.-M., 2008. On the formation and growth of atmospheric nanoparticles. Atmospheric Research 90, 132-150.

Kulmala, M., Lehtinen, K.E.J., Laaksonen, A., 2006. Cluster activation theory as an explanation of the linear dependence between formation rate of 3nm particles and sulphuric acid concentration. Atmos. Chem. Phys. 6, 787-793.

Kulmala, M., Luoma, K., Virkkula, A., Petäjä, T., Paasonen, P., Kerminen, V.-M., Nie, W., Qi, X., Shen, Y., Chi, X., Ding, A., 2016. On the mode-segregated aerosol particle number concentration load: contributions of primary and secondary particles in Hyytiälä and Nanjing. BOREAL ENVIRONMENT RESEARCH 21, 319-331.

Kulmala, M., Vehkamäki, H., Petäjä, T., Dal Maso, M., Lauri, A., Kerminen, V.M., Birmili, W., McMurry, P.H., 2004. Formation and growth rates of ultrafine atmospheric particles: a review of observations. Journal of Aerosol Science 35, 143-176.

Kumar, P., Morawska, L., Birmili, W., Paasonen, P., Hu, M., Kulmala, M., Harrison, R.M., Norford, L., Britter, R., 2014. Ultrafine particles in cities. Environment international 66, 1-10.

Larsen, L.C., Austin, J., Dolislager, L., Lashgari, A., McCauley, E., Motallebi, N., Tran, H., 2003. THE OZONE WEEKEND EFFECT IN CALIFORNIA. California Environmental Protection Agency.

Lin, W., Xu, X., Ge, B., Liu, X., 2011. Gaseous pollutants in Beijing urban area during the heating period 2007–2008: variability, sources, meteorological, and chemical impacts. Atmospheric Chemistry and Physics 11, 8157-8170.

Lin, W., Xu, X., Zhang, X., Tang, J., 2008. Contributions of pollutants from North China Plain to surface ozone at the Shangdianzi GAW Station. Atmos. Chem. Phys. 8, 5889-5898.

Mejia, J.F., Morawska, L., Mengersen, K., 2008. Spatial variation in particle number size distributions in a large metropolitan area. Atmos. Chem. Phys. 8, 1127-1138.

Minoura, H., Takekawa, H., 2005. Observation of number concentrations of atmospheric aerosols and analysis of nanoparticle behavior at an urban background area in Japan. Atmospheric Environment 39, 5806-5816.

Mishra, V.K., Kumar, P., Van Poppel, M., Bleux, N., Frijns, E., Reggente, M., Berghmans, P., Int Panis, L., Samson, R., 2012. Wintertime spatio-temporal variation of ultrafine particles in a Belgian city. Sci Total Environ 431, 307-313.

Monks, P.S., 2000. A review of the observations and origins of the spring ozone maximum. Atmospheric Environment 34, 3545-3561.

Morawska, L., Ristovski, Z., Jayaratne, E.R., Keogh, D.U., Ling, X., 2008. Ambient nano and ultrafine particles from motor vehicle emissions: Characteristics, ambient processing and implications on human exposure. Atmospheric Environment 42, 8113-8138.

Oberdorster, G., Sharp, Z., Atudorei, V., Elder, A., Gelein, R., Kreyling, W., Cox, C., 2004. Translocation of inhaled ultrafine particles to the brain. Inhalation toxicology 16, 437-445.

Pérez, N., Pey, J., Cusack, M., Reche, C., Querol, X., Alastuey, A., Viana, M., 2010. Variability of Particle Number, Black Carbon, and PM10, PM2.5, and PM1Levels and Speciation: Influence of Road Traffic Emissions on Urban Air Quality. Aerosol Science and Technology 44, 487-499.

Petzold, A., Ogren, J.A., Fiebig, M., Laj, P., Li, S.M., Baltensperger, U., Holzer-Popp, T., Kinne, S., Pappalardo, G., Sugimoto, N., Wehrli, C., Wiedensohler, A., Zhang, X.Y., 2013. Recommendations for reporting "black carbon" measurements. Atmospheric Chemistry and Physics 13, 8365-8379.

R Core Team, D., 2015. R: a Language and Environment for Statistical Computing., R Foundation for statistical computing, Vienna, Austria.

Reche, C., Querol, X., Alastuey, A., Viana, M., Pey, J., Moreno, T., Rodríguez, S., González, Y., Fernández-Camacho, R., de la Rosa, J., Dall'Osto, M., Prévôt, A.S.H., Hueglin, C., Harrison, R.M., Quincey, P., 2011. New considerations for PM, Black Carbon and particle number concentration for air quality monitoring across different European cities. Atmospheric Chemistry and Physics 11, 6207-6227.

Ripoll, A., Pey, J., Minguillón, M.C., Pérez, N., Pandolfi, M., Querol, X., Alastuey, A., 2014. Three years of aerosol mass, black carbon and particle number concentrations at Montsec (southern Pyrenees, 1570 m a.s.l.). Atmospheric Chemistry and Physics 14, 4279-4295.

Rodríguez, S., Cuevas, E., 2007. The contributions of "minimum primary emissions" and "new particle formation enhancements" to the particle number concentration in urban air. Journal of Aerosol Science 38, 1207-1219.

Rodríguez, S., Cuevas, E., González, Y., Ramos, R., Romero, P.M., Pérez, N., Querol, X., Alastuey, A., 2008. Influence of sea breeze circulation and road traffic emissions on the relationship between particle number, black carbon, PM1, PM2.5 and PM2.5–10 concentrations in a coastal city. Atmospheric Environment 42, 6523-6534.

Rodríguez, S., Dingenen, R.V., Putaud, J.P., Dell'Acqua, A., Pey, J., Querol, X., Alastuey, A., Chenery, S., Ho, K.-F., Harrison, R.M., Tardivo, R., Scarnato, B., Gemelli, V., 2007. A study on the relationship between mass concentrations, chemistry and number size distribution of urban fine aerosols in Milan, Barcelona and London. Atmos. Chem. Phys. 7, 2217-2232.

Rose, D., Wehner, B., Ketzel, M., Engler, C., Voigtlander, J., Tuch, T., Wiedensohler, A., 2006. Atmospheric number size distributions of soot particles and estimation of emission factors. Atmos. Chem. Phys. 6, 1021-1031.

Schwarz, J.P., Gao, R.S., Spackman, J.R., Watts, L.A., Thomson, D.S., Fahey, D.W., Ryerson, T.B., Peischl, J., Holloway, J.S., Trainer, M., Frost, G.J., Baynard, T., Lack, D.A., de Gouw, J.A., Warneke, C., Del Negro, L.A., 2008. Measurement of the mixing state, mass, and optical size of individual black carbon particles in urban and biomass burning emissions. Geophysical Research Letters 35.

Shi, J.P., Evans, D.E., Khan, A.A., Harrison, R.M., 2001. Sources and concentration of nanoparticles (<10nm diameter) in the urban atmosphere. Atmospheric Environment 35, 1193-1202.

Shi, J.P., Khan, A.A., Harrison, R.M., 1999. Measurements of ultrafine particle concentration and size distribution in the urban atmosphere. The Science of the Total Environment 235, 51-54.

Shi, J.P., Mark, D., Harrison, R.M., 2000. Characterization of Particles from a Current Technology Heavy-Duty Diesel Engine. Environ. Sci. Technol 34, 748-755.

Voigtländer, J., Tuch, T., Birmili, W., Wiedensohler, A., 2006. Correlation between traffic density and particle size distribution in a street canyon and the dependence on wind direction. Atmos. Chem. Phys. 6, 4275-4286.

von Bismarck-Osten, C., Birmili, W., Ketzel, M., Massling, A., Petäjä, T., Weber, S., 2013. Characterization of parameters influencing the spatio-temporal variability of urban particle number size distributions in four European cities. Atmospheric Environment 77, 415-429.

Weber, S., Kordowski, K., Kuttler, W., 2013. Variability of particle number concentration and particle size dynamics in an urban street canyon under different meteorological conditions. Sci Total Environ 449, 102-114.

Wehner, B., Uhrner, U., von Löwis, S., Zallinger, M., Wiedensohler, A., 2009. Aerosol number size distributions within the exhaust plume of a diesel and a gasoline passenger car under on-road conditions and determination of emission factors. Atmospheric Environment 43, 1235-1245.

Wehner, B., Wiedensohler, A., 2003. Long term measurements of submicrometer urban aerosols: statistical analysis for correlations with meteorological conditions and trace gases. Atmos. Chem. Phys. 3, 867-879.

Yoo, J.M., Jeong, M.J., Kim, D., Stockwell, W.R., Yang, J.H., Shin, H.W., Lee, M.I., Song, C.K., Lee, S.D., 2015. Spatiotemporal variations of air pollutants (O₃, NO₂, SO₂, CO, PM₁₀, and VOCs) with land-use types. Atmospheric Chemistry and Physics 15, 10857-10885.

Zhu, Y., Hinds, W.C., Kim, S., Sioutas, C., 2002. Concentration and Size Distribution of Ultrafine Particles Near a Major Highway. Journal of the Air & Waste Management Association 52, 1032-1042.

Table 1: Air quality instrumentation at Leicester AURN site during the sampling period.

Air quality parameters	Monitors
PNC (six size bins)	UFP Monitor TSI 3031 (~20-200nm)
TNC	WCPC TSI Model 3783 (7-1000nm)
NO, NO_2, NO_X	Teledyne API Model T200 Chemiluminescence NO/NO2/NOX Analyzer
eBC	MAAP (Thermo Scientific 5012) with $PM_{2.5}$ inlet
$PM_{2.5}$	TEOM-FDMS
CO	Teledyne API Model T300U Trace-level Gas Filter Correlation CO Analyzer (IR Absorption)
O_3	UV absorption

Table 2: Values of the slopes S1 and S2 found at AURN site. S1 and S2 are expressed as 10^6 particles/ng eBC (for definitions see text).

Time of the day		S1	S2
All day	00.00-23:00 h	2.25	28.60
Night	00:00-04:00 h	2.16	32.05
Morning	07:00-09:00 h	2.53	18.15
Midday	11:00-14:00 h	2.85	36.4
Evening	17:00-20:00 h	2.75	24.35

Table 3: Summary of S1 and S2 values found during rush hours in previous studies and this study.

Location	S1 ($\times 10^6$) (particles /ng eBC)	S2 ($\times 10^6$) (particles /ng eBC)	Study
Milan	4.75	47	Rodriguez and Cuevas, 2007
Huelva	6.9	148	Fernández-Camacho et al., 2010
Santa Cruse de Tenerife	7.9	30.3	González et al., 2011
London	2.9	6.3	Reche et al., 2011
Lugano	3.1	20.9	Reche et al., 2011
Bern	3.6	18.9	Reche et al., 2011
Barcelona	5.1	24.5	Reche et al., 2011
Hyytiälä	1.28	-	Kulmala et al., 2016
Nanjing	1.67	-	Kulmala et al., 2016
Leicester	2.53	18.15	This study

Table 4: Total mean percentage of N1 and N2 for daily and midday-afternoon at the AURN site (2014-2015).

Time of the day		N1%	N2%
All day	00.00-23:00 h	43	57
Night	00:00-04:00 h	39	61
Morning	07:00-09:00 h	49	51
Midday	11:00-14:00 h	38	62
Evening	17:00-20:00 h	46	54

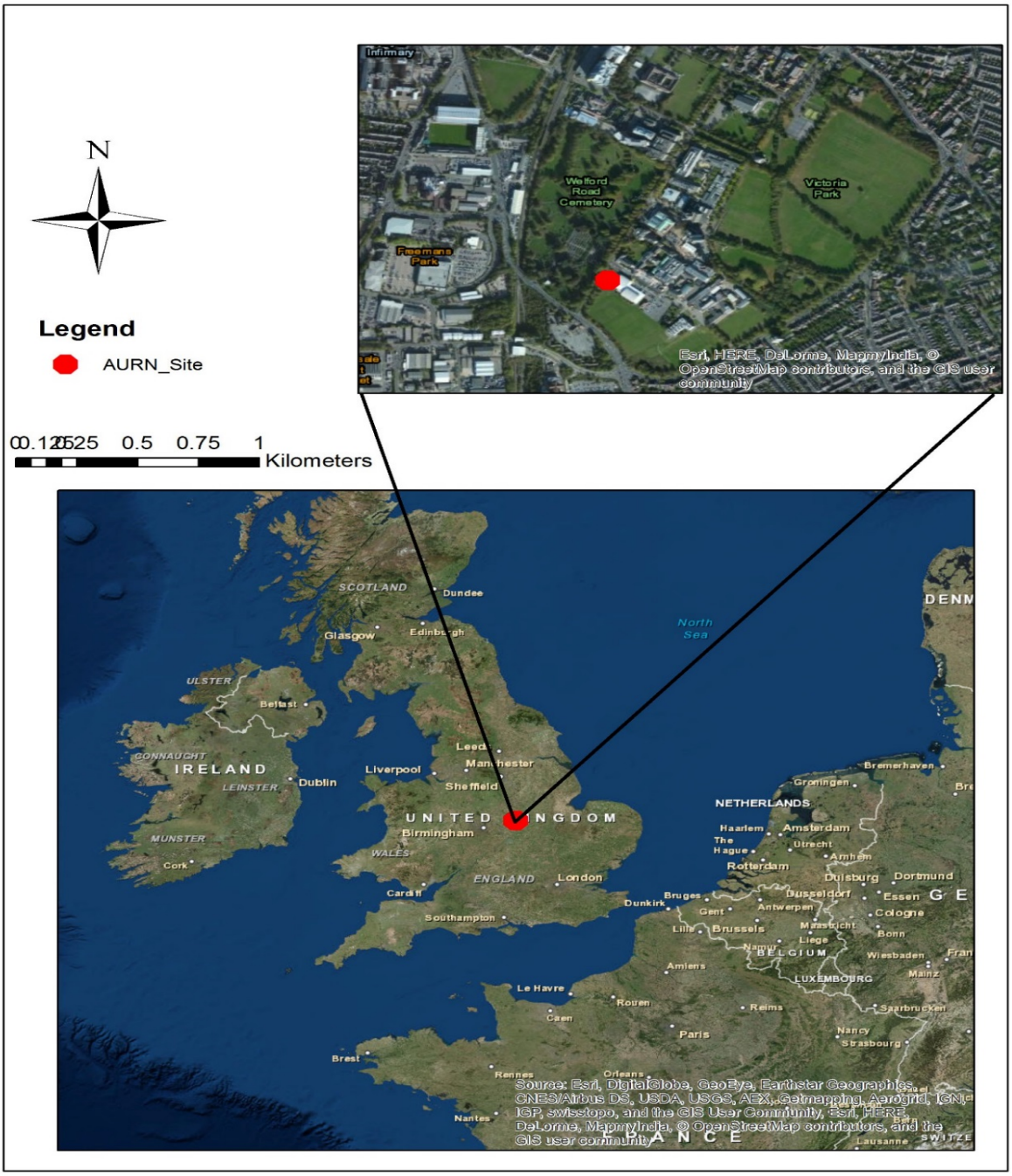

Figure 1: Leicester and location of the sampling site (denoted AURN)

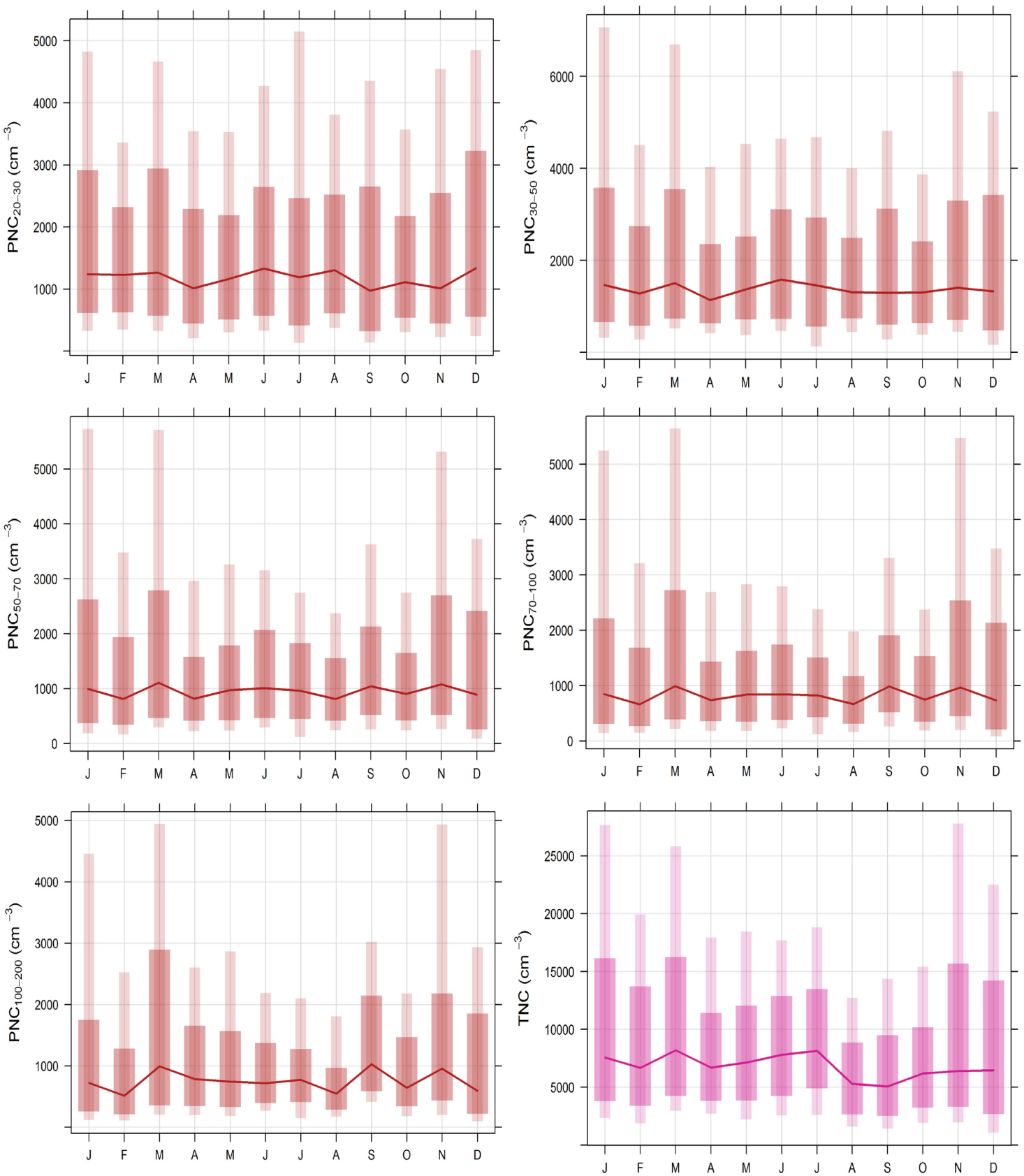

Figure 2: Monthly variations in the median, 25/75th and 5/95th quantile values for PNC size classes, and TNC for 2014 at AURN site.

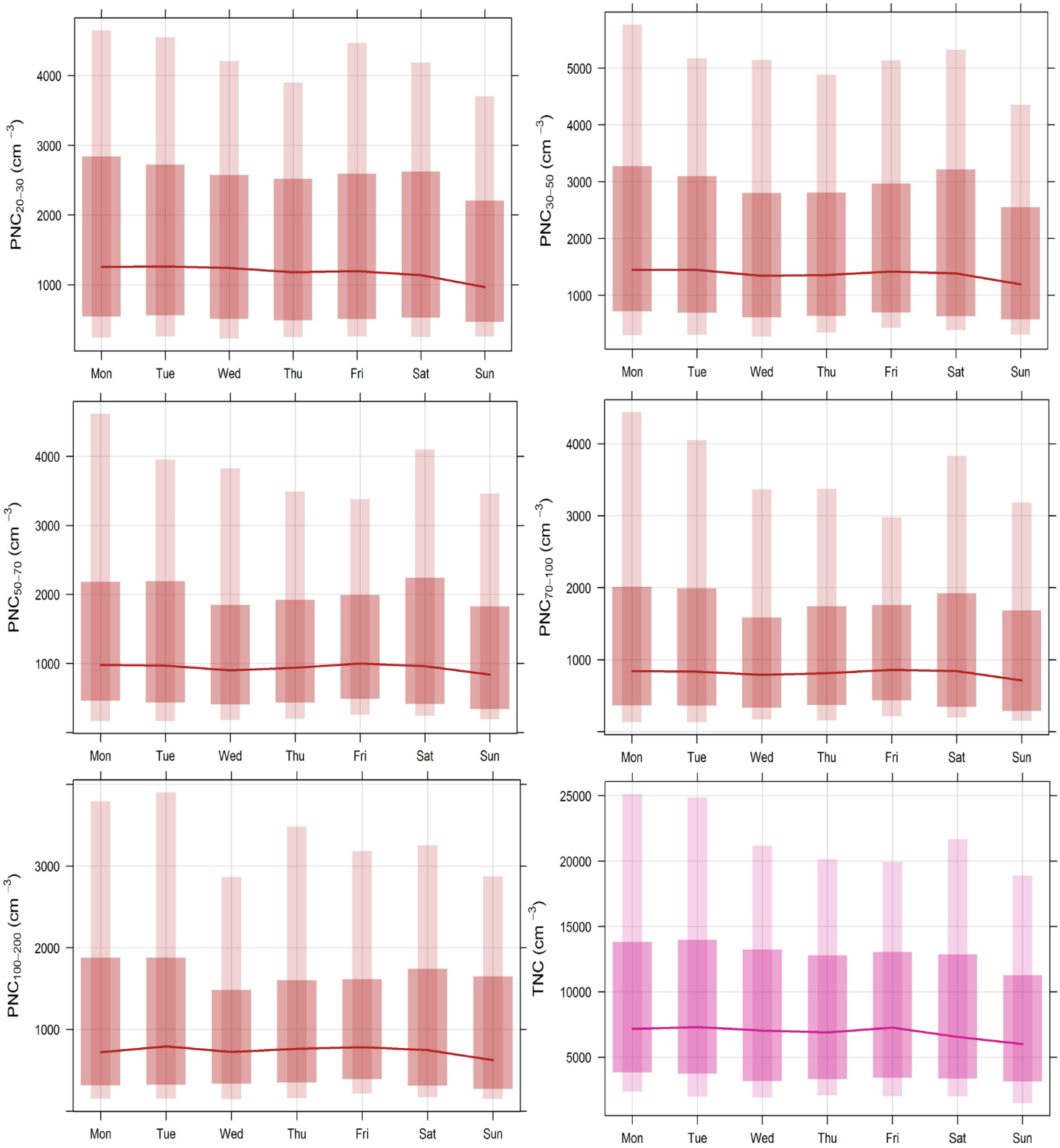

Figure 3: Daily variations in the median, 25/75th and 5/95th quantile values for PNC size classes, and TNC for 2014 at the AURN site.

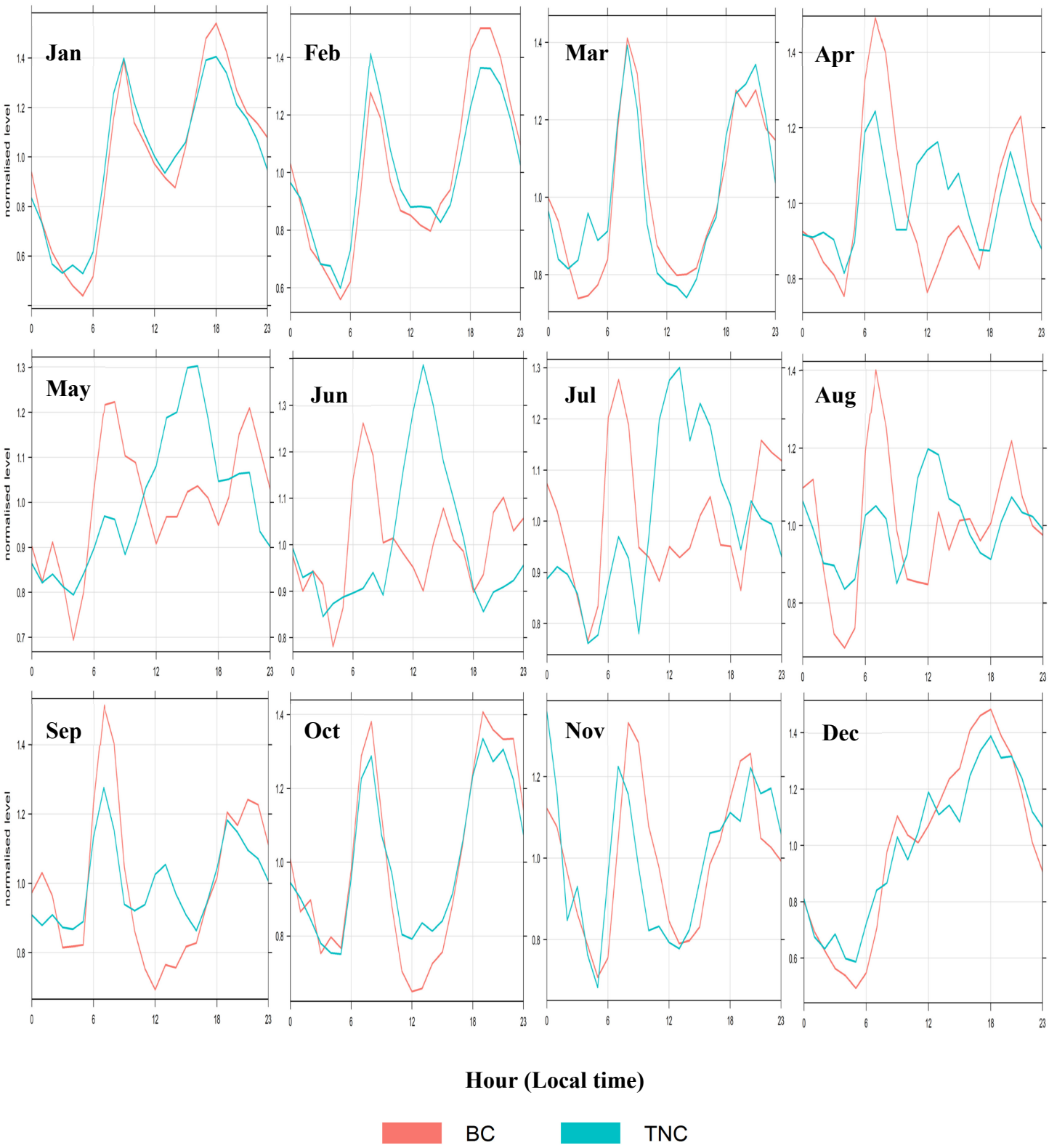

Figure 4: : Diurnal variations of eBC, and TNC concentrations for each month in 2015.

749

750

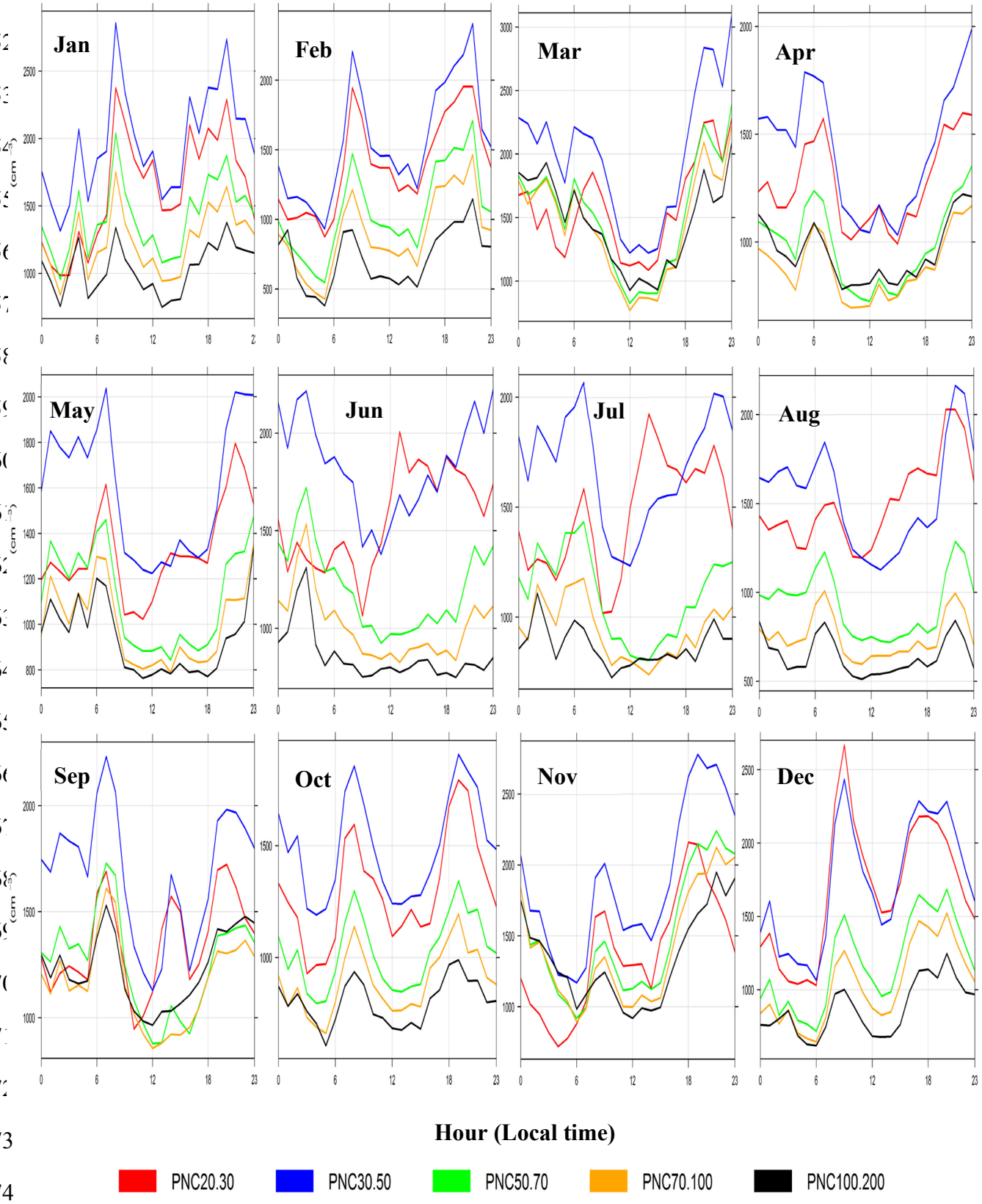

Figure 5: Diurnal variations of different size channel of PNC for each month in 2014.

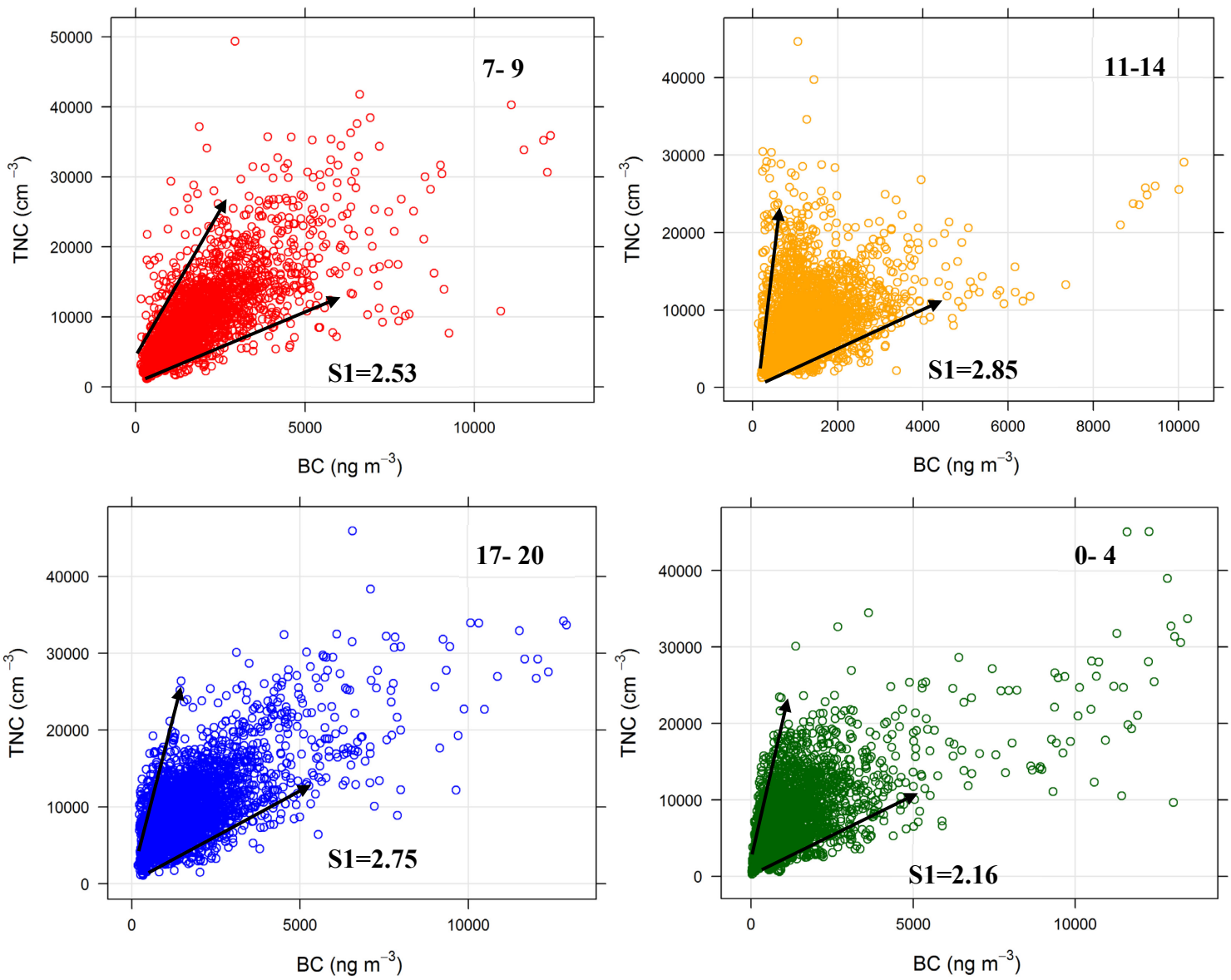

Figure 6: Half-hourly mean values of TNC versus eBC concentrations at different times of the day in Leicester. S1 (10^6 particles per ng eBC).

777

778

779

780

781

782

783

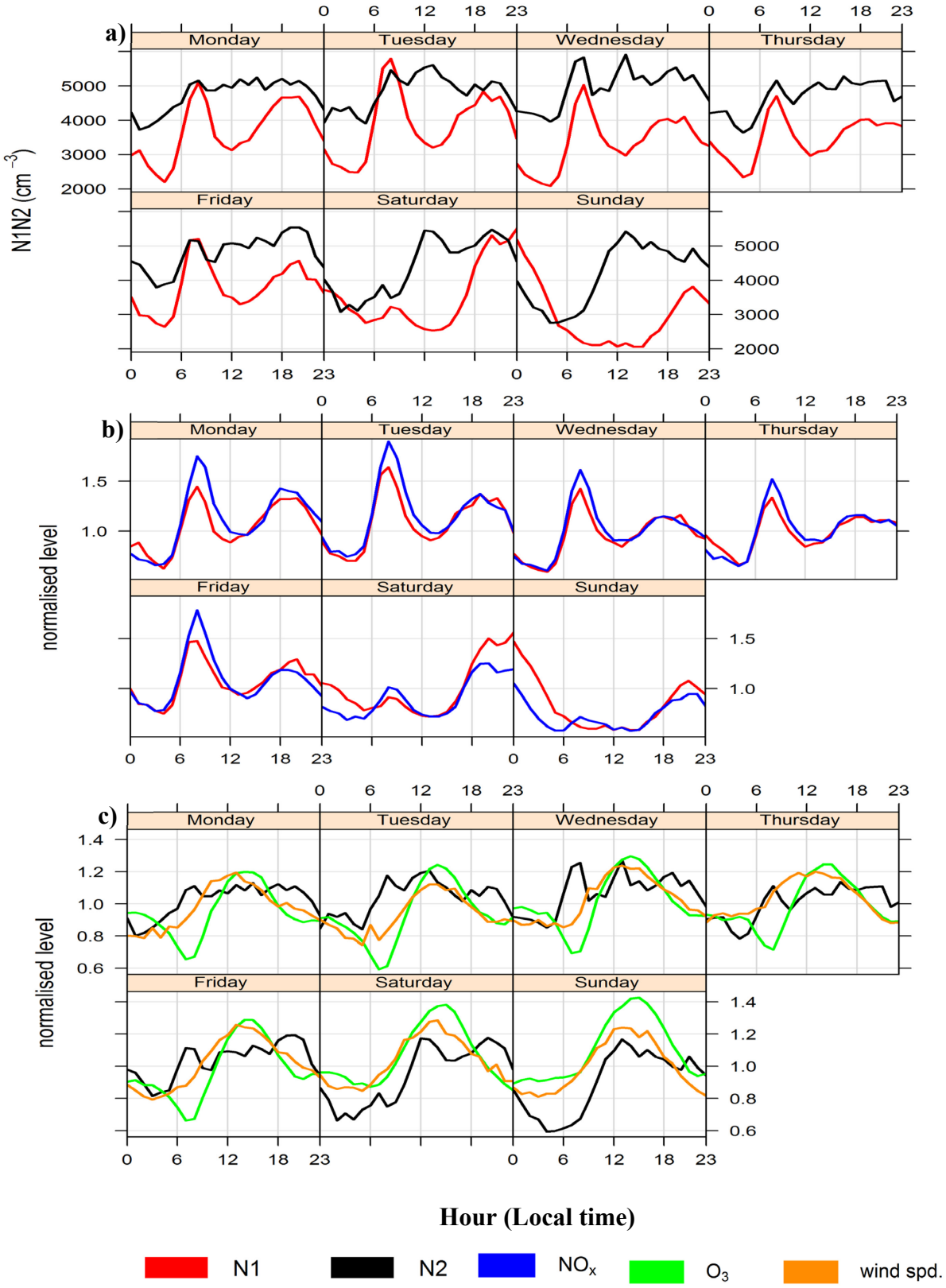

Figure 7: Half-hourly mean values of N1, N2, the gaseous pollutants (NOx, O^3, µg m^{-3}) concentrations and the wind speed (m s^{-1}) for every day of the week.

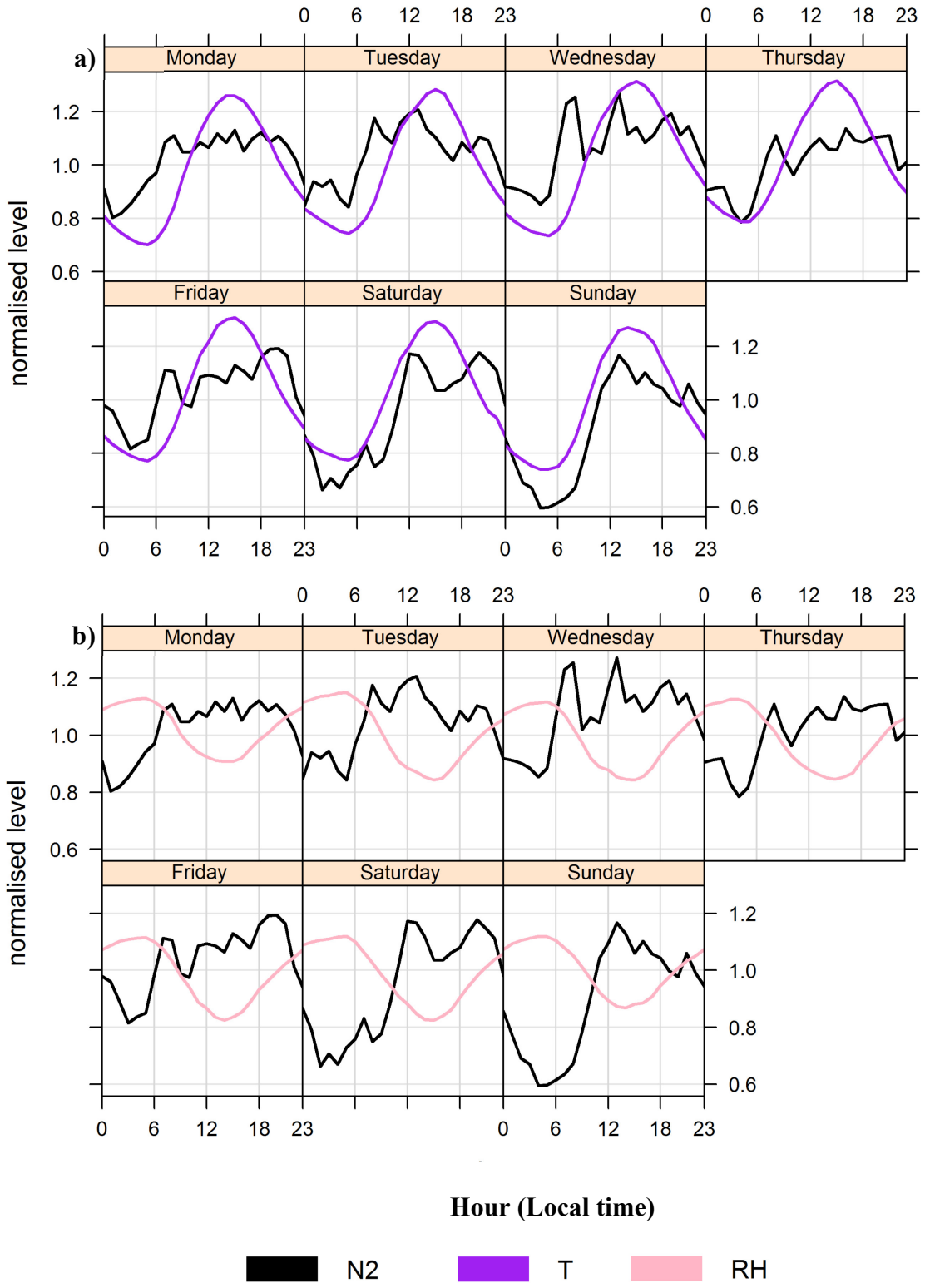

Figure 8: Half-hourly mean values of N2 (cm-3), the temperature (T, ºC) and the relative humidity (RH, %) for every day of the week.

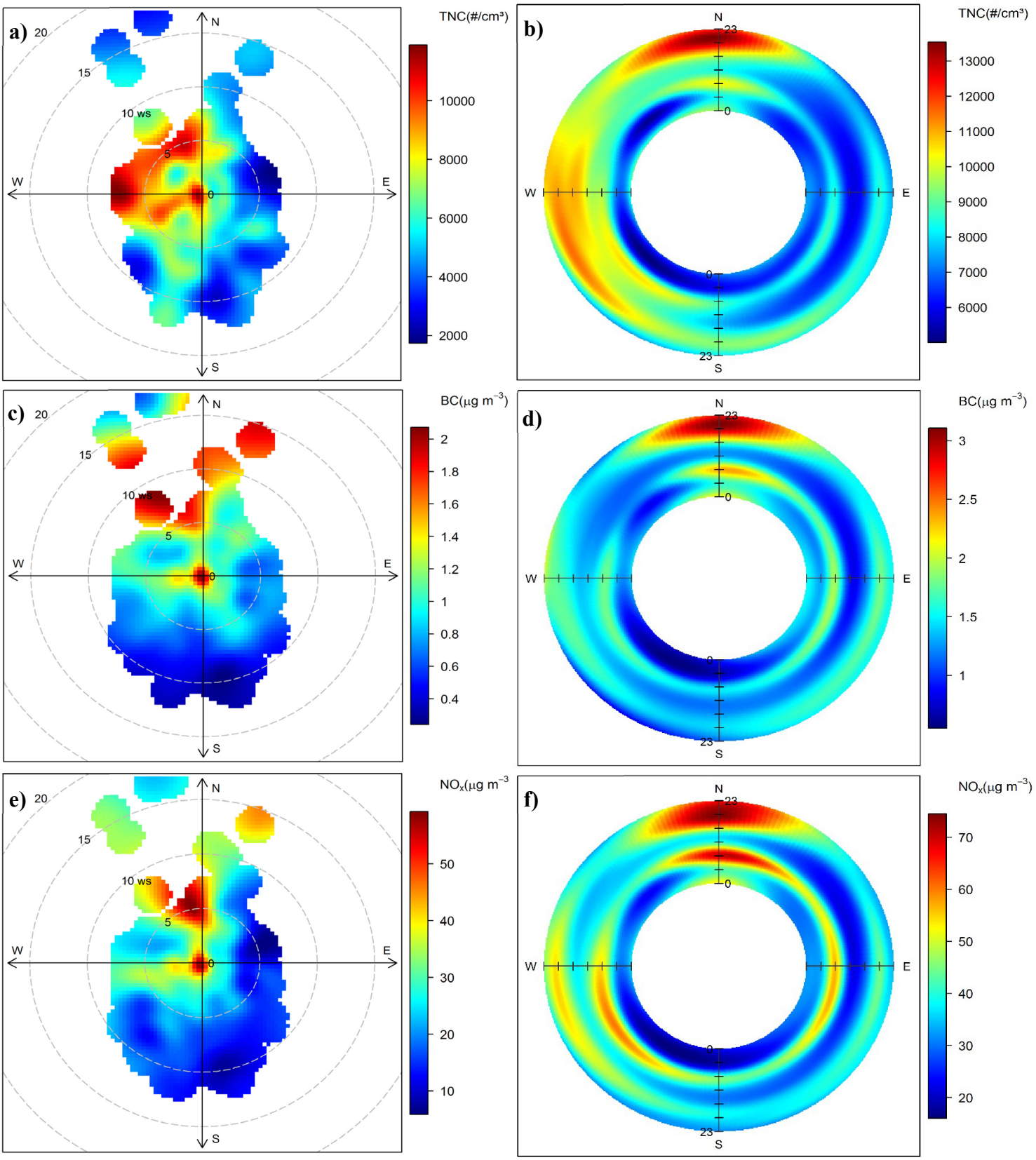

Figure 9: Bivariate polar plots of a) TNC, c) eBC, and e) NOx concentrations, respectively at the AURN site. The centre of each plot represents a wind speed of zero, which increases radially outward. The concentrations are shown by the colour scale. Polar annulus plots of b) TNC, d) eBC, and f) NOx concentrations, respectively at the AURN site. Inside of circle is 00:00-01:00 h running through the day to 23:00-24:00.

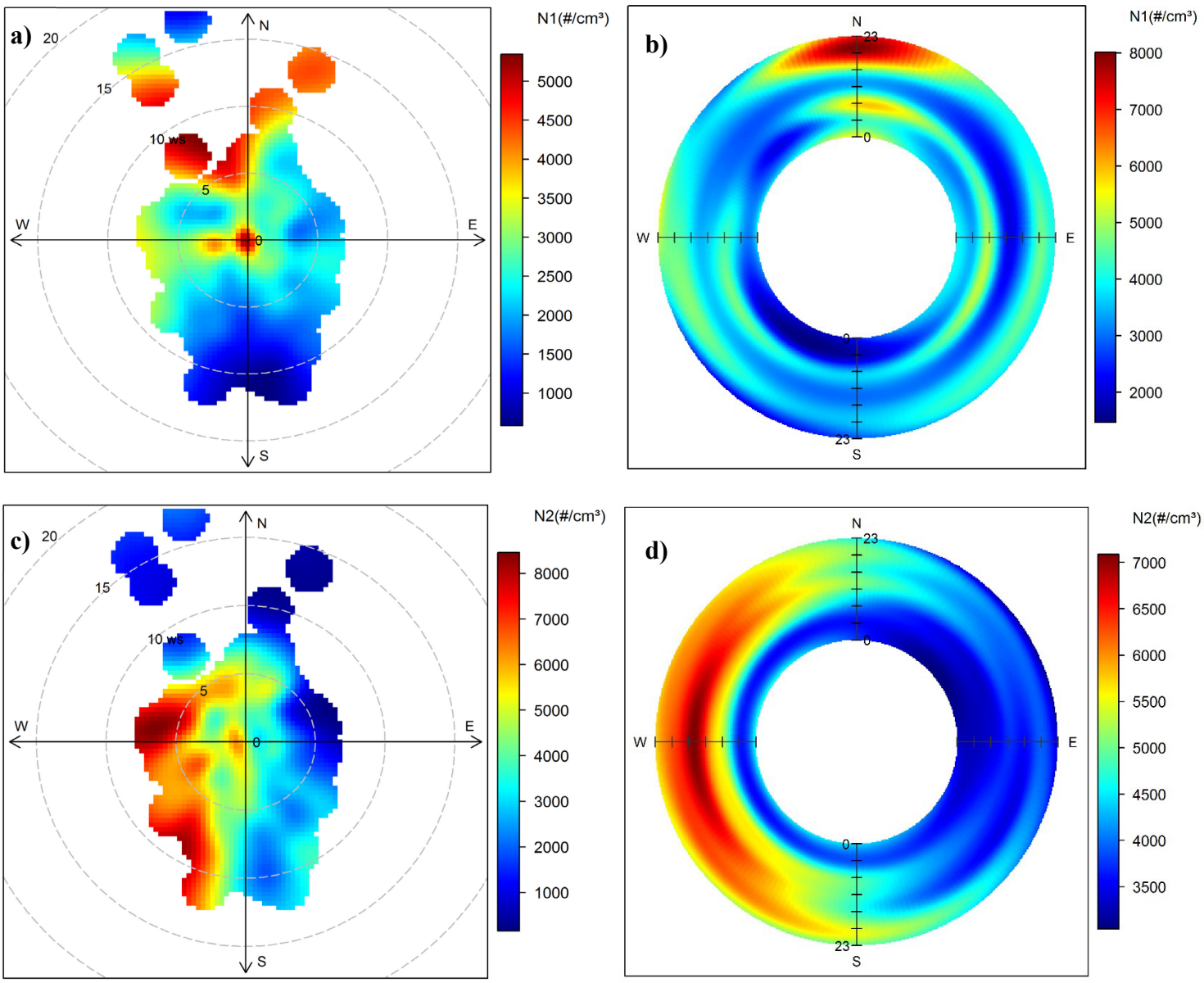

Figure 10: Bivariate polar plots of a) N1, and c) N2, concentrations, respectively at the AURN site. The centre of each plot represents a wind speed of zero, which increases radially outward. The concentrations are shown by the colour scale. Polar annulus plots of b) N1, and d) N2, concentrations, respectively at the AURN site. Inside of circle is 00:00-01:00 h running through the day to 23:00-24:00.

787

788